THE AMERICAN SOCIETY OF MECHANICAL ENGINEERS
345 E. 47 St., New York, N.Y. 10017

92-G

Experimental Study on the Three Dimensional Flow Within a Compressor Cascade with Tip Clearance: Part I—Velocity and Pressure Fields

SHUN KANG* and CH. HIRSCH**

Vrije Universiteit Brussel, Department of Fluid Mechanics
Pleinlaan 2, 1050 Brussel, Belgium

Abstract

Experimental results from a study of the 3-D flow in a linear compressor cascade with stationary endwall at design conditions are presented for tip clearance levels of 1.0, 2.0 and 3.3 percent of chord, compared with the no clearance case. In addition to five-hole probe measurements, extensive surface flow visualizations are conducted. It is observed that for the smaller clearance cases a weak horseshoe vortex forms in the front of the blade leading edge. At all the tip gap cases, a multiple tip vortex structure with three discrete vortices around the midchord is found.The tip leakage vortex core is well defined after the midchord but does not cover a significantly great area in traverse planes. The presence of the tip leakage vortex results in the passage vortex moving close to the endwall and to the suction side.

Nomenclature

c	= blade chord
C_p	= static pressure
H	= shape factor
l	= blade span
LE	= leading edge
PS	= pressure side
P_y	= coordinate of the passage vortex centre from low wall
P_z	= coordinate of the passage vortex centre from suction side
s	= pitch
SS	= suction side
TE	= trailing edge
u, u_a	= axial velocity, mass-averaged axial velocity
V_1	= inlet resultant velocity
x, y, z	= axial, spanwise and pitchwise distance
δ	= boundary layer thickness
δ^*	= displacement thickness

* Ph D. Student, Permanent address: Power Engineering Dept., Harbin Institute of Technology, Harbin 150006, P. R. China

** Professor, Member ASME

Introduction

Research on the three dimensional flow in axial turbomachinery with tip gap can be traced back to the 1920's as reviewed by Prasad (1977). Most of the investigations on axial compressor flow fields have been concerned with rotor wake characteristics (Lakshminarayana and Poncet, 1974; Hirsch and Kool, 1977; Kool et al., 1978) and with the interaction region of the casing wall boundary layer, the wake and the tip leakage flow (Davino and Lakshminarayana, 1982; Hunter and Cumpsty, 1982). The behaviour of the flow fields inside and behind an axial rotor has been examined by Dring et al. (1982, 1985) and Inoue and Kuroumaru (1984). Experiment studies with special emphasis on the leakage flow development near and in the tip clearance have been conducted by Bindon (1986a and b) and Moore and Tilton (1988) for linear turbine cascade, and by Lakshminarayana, et al. (1982 and 1987), Inoue et al. (1989 and 1991), Storer and Cumpsty (1991) for axial compressors. The tip leakage flow and its subsequent rolling up into a vortex have been clearly demonstrated and described originally by Rains (1954) and subsequently by Lakshminarayana (1970). More recently, Chen et al. (1991), based on the slender body theory in external aerodynamics, proposed an approximate method for analyzing compressor tip clearance flow. Numerical computation of the three dimensional flow in a passage with tip clearance has also been reported recently (Hah, 1986; Storer and Cumpsty, 1991) using the Navier-Stokes equations, showing satisfactory prediction on both the overall effects and certain local details near and inside the tip clearance. But for further validation of the computational codes, detailed measured data and physical interpretations are imperative.

The present paper intends to show more information on the secondary flow and vorticity within and behind a linear compressor cascade, with tip clearance, of NACA 65-1810 blade profile at design conditions, and to present the overall features of the tip leakage vortex, such as the evolution of its size, centre position and vorticity. The investigation is presented in two parts. In this part, Part I, the overall secondary flows, total pressure losses and static pressures are discussed; in part II, the main attention will be focused on the vorticity field.

Experimental Facility and Instrumentation

The experimental facility, instrumentation and measurement accuracy have been described by Kang and Hirsch (1991). Hence only a short review is presented here.

Presented at the International Gas Turbine and Aeroengine Congress and Exposition
Cologne, Germany June 1-4, 1992
This paper has been accepted for publication in the Transactions of the ASME
Discussion of it will be accepted at ASME Headquarters until September 30, 1992

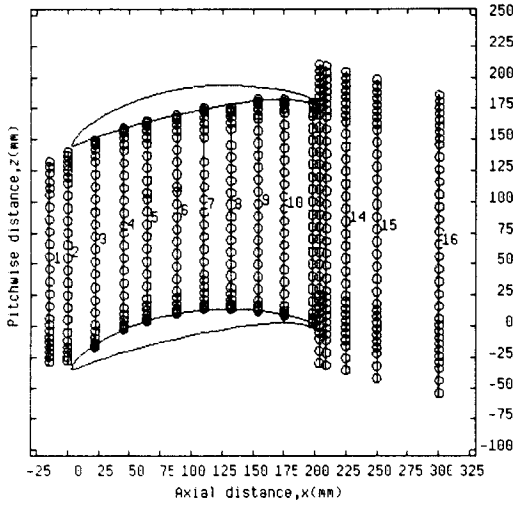

Fig.1 Cascade coordinate system and traverse measurement point distribution in a spanwise (y axis) section

The present investigations were carried out in the low speed compressor cascade wind tunnel of the Department of Fluid Mechanics, Vrije Universiteit Brussel (VUB). The test section of the wind tunnel consists of two parallel end plates, aligned horizontally, between which a cascade with seven NACA 65-1810 blades is installed. The blades, with flat tips, are cantilivered from the upper wall of the cascade. The lower wall, supported by four screws and stiffed horizontally by other four screws, can be adjusted to produce tip clearance with an uncertainty of ±0.1mm for the seven tip gaps. The tip clearance spaces in the present study were 1.0, 2.0 and 3.3% of chord. The periodicity is shown from the uncertainty of the static pressure coefficients on the lower wall of the leading and trailing edges of the measured passage, for 2.0% clearance as an example, it is better than 1%. The blade aspect ratio is 1.0.

Traverse measurements with a five hole probe were conducted, at tip clearance of 1.0 and 2.0%, in the passage with the middle blade as its pressure side. There were 16 traverse planes (Fig.1) from 7.5% chord upstream of the leading edge to 50% chord downstream of the cascade exit plane. In each of the traverse planes 24 stations from suction side to pressure side and 33 stations behind the cascade were arranged. Fifteen points in each station are recorded from near the endwall to midspan. In order to obtain some information on the flow in the whole span region, more points (26 points in span) are taken in the traverse plane No.14 for 1.0% tip clearance, covering 98% of the span.

The five hole probe with external size of 2.6mm is mounted on a support which is located downstream and fixed to the upper wall of the cascade, from which the probe can be inserted into the flow field. The static pressures of blade surfaces and endwall were also recorded by static pressure tubes.

The five-hole probe was fully calibrated in a jet, Kang (1989). The accuracies of the measured velocity and total pressure are 1% of the inlet midspan values from where all the reference parameters were taken. The uncertainty of the measured flow direction is better than 1°.

The methods used for visualizing the three dimensional flow inside the linear compressor cascade included oil film and titanium dioxide, cotton threads, white paint-trace and black ink-trace. For the last two methods, a very thin plastic paper was pasted on the visualized surface; photos were taken after tearing it off. All the flow visualization studies had been filmed in motion with a video camera. The visualization studies are conducted on the clearances of 0.0 to 3.3%.

Test Conditions

With the tip clearances, all the inlet flow conditions, except the dynamic pressure, were not significantly different from those without tip clearance reported by Kang and Hirsch (1991). The test Reynolds number, based on blade chord was about 2.9×10^5; free stream turbulence intensity was 3.4%. The mass-averaged air inlet and outlet angles, measured 40 % chord upstream and 25% chord downstream were 29.3° and -2.5°, compared to the design values of 30° and -4.02°, respectively. The inlet boundary layer was turbulent. The integral parameters of the inlet endwall boundary layer, at 40% chord upstream of the leading edge, are summarized as follow:

$\delta/c = 0.2$ $\quad\quad$ $\delta^*/c = 0.144$

$\theta/c = 0.118$ $\quad\quad$ $H = 1.22$

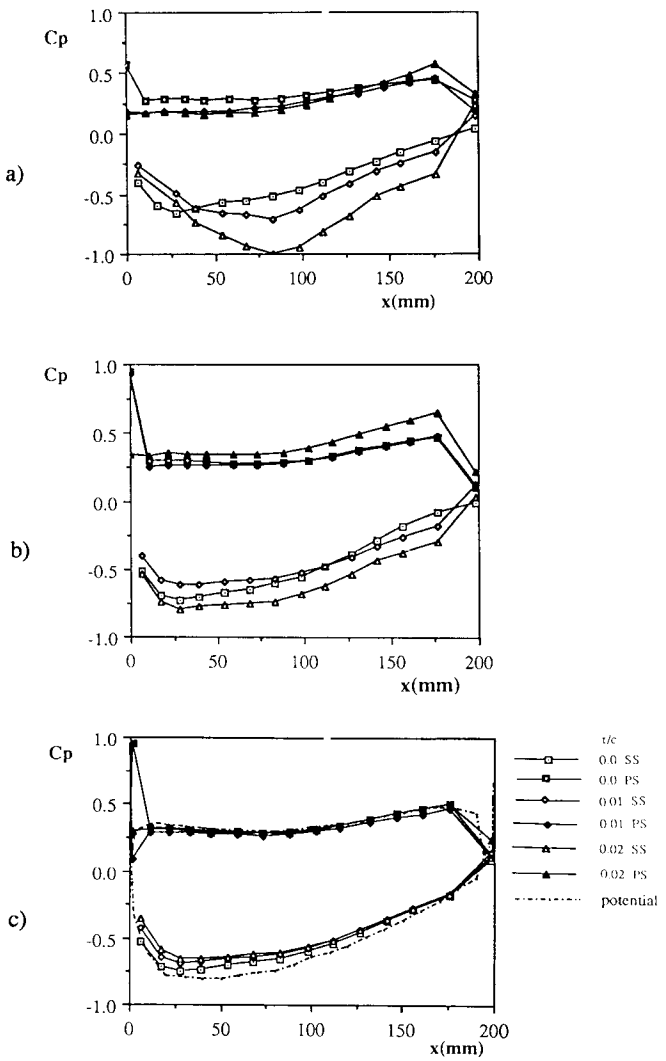

Fig.2 Static pressure distribution on blade surface in three span positions, a) 1.5%, b) 15% and c) midspan

Static Pressure Distribution on Blade Surfaces

The measured static pressure distributions on the blade surfaces at three spanwise positions, y/l=0.015, 0.15 and 0.5 (midspan), are

given in Fig.2 for tip clearances, 0.0, 1.0 and 2.0% chord with potential calculation. The values closest to the trailing edge were obtained from the five probe readings at the measured point near the blade surfaces on traverse plane No.11, 2mm ahead of the exit plane. It is seen from Fig.2b and 2c that the pressure distributions at the spanwise positions far away from the blade tip (15% and midspan) have qualitatively similar shapes for different tip clearances with some change in the pressure values, especially in the first half chord on the suction surface. The shift, resulting in unloading, may be caused by the motion of the tip leakage flow, which is to be expected as the midspan is just a half blade chord away from the tip. As in the case without tip gap, the pressure peaks on the suction surface with tip clearances are also located at about 15 percent chord downstream of the leading edge at 15% span and midspan.

Near the blade tip (Fig.2a), however, the static pressure distribution is significantly different from the other spanwise positions. In the vicinity of the leading edge, it shows small unloading, then, strong reloading takes place around the midchord. Undoubtedly, this is related to the generation of the tip leakage flow and the motion of the corresponding tip leakage vortex. The pressure increase on the suction side near the leading edge is due to the interaction with the fluid passing through the tip gap from the pressure side, where the tip leakage vortex originates, see later discussions. The increment of blade force, from 20% chord downstream of the leading edge, results from the low pressure core of the tip leakage vortex. A similar behaviour has been mentioned by Graham (1986) in his investigation of a tip clearance cascade in a water rig, with larger gaps.

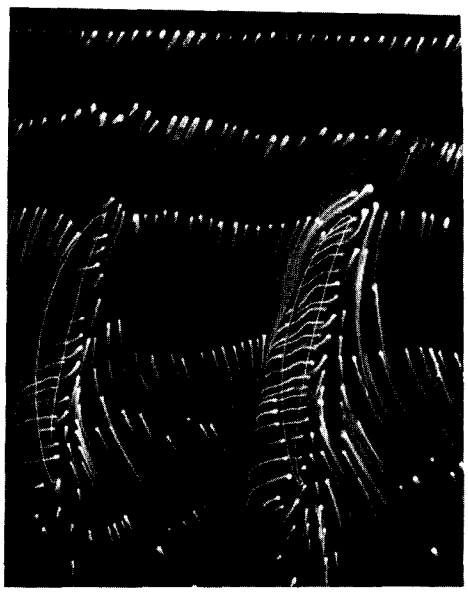

Fig.3 Paint-trace visualization on the endwall, at 2.0% tip clearance

Surface Flow Visualization

Extensive visualizations for 0.0, 1.0, 2.0 and 3.3% clearance have been analysed in detail and reported by Kang (1991b). In this paper only the analysis referring to the 2.0% clearance will be presented.

Figure 3 shows the paint-trace pattern of the endwall around and under the blades and Fig.4 shows the ink-trace pattern of a blade tip surface. The topological patterns of the endwall and blade surface skin-friction lines or limiting streamlines, deduced from the visualizations, are respectively shown in Fig.5 and 6.

Endwall Flow Pattern As seen from Fig.3, the skin-friction line, approaching the blade leading edge, splits into two branches at a point in front of the leading edge. This is a saddle point, labelled S_h in

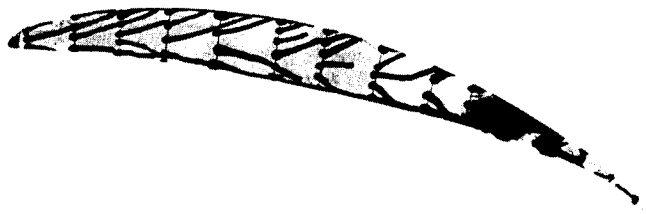

Fig.4 Ink-trace visualization on the blade tip surface, at 2.0% tip clearance

Fig.5 Schematic of the flow pattern on the wall at $\tau/c=0.02$

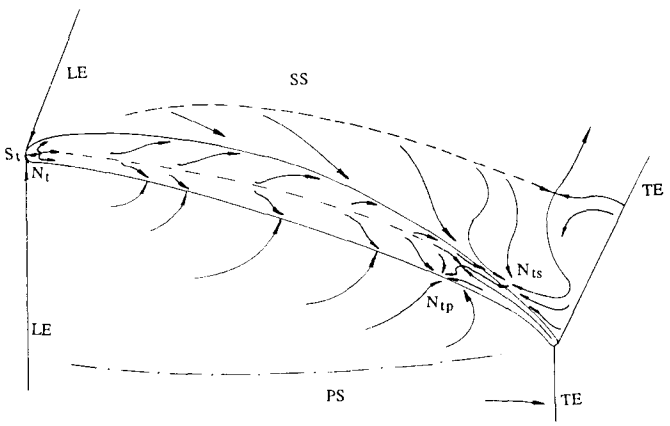

Fig.6 Schematic of the flow pattern on the blade tip, with 'opened-up' pressure and suction surfaces

Fig.5, resulting in the formation of a leading edge horseshoe vortex. Its suction side branch turns around the leading edge and joins with the separation line of the tip leakage vortex at about 25% chord downstream. The pressure side branch stretches toward downstream a short distance, then changes its direction at about 5% chord, finally passes through the tip gap and tends to join with the suction side branch. Sjolander and Amrud (1987) also found, at their smaller clearance (τ/c=0.96%) of a turbine cascade, that the pressure side leg of the vortex was swept back over the blade tip with the first 10% of chord length. This effect was, however, not seen for the 1.0% tip clearance, where the pressure side branch stretches always toward downstream, similar as for zero clearance. Increasing the tip size to 3.3%, the saddle point S_h disappeared and no sight of a leading edge horseshoe vortex could be seen.

The deepest impression on Fig.3 is the formation of a reattachment line near the pressure side and a separation line near the suction side, as respectively sketched by L_r and L_L in Fig.5. The line L_L is the separation line of the tip leakage vortex. From a detailed analysis of the visualizations, a separation line close to L_L, indicated as P_L on Fig.5, can be identified. The paint-traces around the midpitch converge to this line which is certainly the separation line of the passage vortex. The flow divergence from the reattachment line L_r implies a flow towards the endwall. As a result, a node and a saddle point will be topologically generated at the leading edge region, as shown in Fig.5 by N_L and S_L. Besides, it is seen in Fig.3 that the limiting streamlines issued from the reattachment line L_r towards the pressure side are all going into the gap at almost right angles to the pressure surface except near the leading and the trailing edges where the pressure-driven leakage flows are small.

Even though the origin of the separation line of the tip leakage vortex is not easily identified from Fig.3, the origin might possibly be the saddle point S_L. The apparently rolling-up of the tip leakage vortex starts just downstream of the leading edge in the suction side corner. Inside the gap the vortex may be mixed with the leakage flow.

Blade Surface Flow Pattern One of the new observations in the present visualizations is the flow pattern on the blade tip surface. It is seen from the ink-trace visualization of Fig.4 at 2.0% clearance that the limiting streamlines, diverging from about the middle of the blade profile, converge towards the tip edges over about 70% chord length from the leading edge. Near the trailing edge reverse flow takes place. As a result, a saddle and a node points were formed at the leading edge region, and two nodes divided by a saddle were formed in the region of about 70 to 86% chord as schematically shown in Fig.6 by S_t, N_t, N_{tp} and N_{ts}. Fig.6 shows the schematic flow pattern of the blade tip surface, together with the 'opened-up' pressure and suction surfaces.

From the visualizations on the pressure and suction surfaces, see Kang (1991b) for details, it was observed that near the tip, the paint-traces also converged to the corresponding blade tip edges. These observations are schematically shown in Fig.6. As a result, Figure 7 presents a multiple tip vortex structure based on the visualizations. It consists of the well known tip leakage vortex, a tip separation vortex and a secondary vortex. The convergent line along the suction side edge in Fig.6 may be the separation line of the secondary vortex which has an opposite rotation sense to the tip leakage vortex. The presence and rotation of this vortex can be evidenced from the secondary flow charts in the suction side corner, see Fig.13 and later discussion. The other convergence line along the pressure side edge in Fig.6 may be the separation line of the tip separation vortex. This vortex, in a section, is similar to the so-called separation bubble or vena contracta, as referred by Rains (1954) and Moore and Tilton (1988). However, it is really not a separation bubble but a vortex aligning along the tip. Both of the separation lines along the blade edges are all issued from the saddle point S_t (Fig.4 and 6) at the leading edge and terminated at two nodes N_{tp} and N_{ts} near the trailing edge. These two nodes are generally unstable; they may change from node to degenerated node or spiral node. When they are spiral nodes, the oil, converged to the separation lines and stacked around the singular points, was shed into the flow field, as can be seen also from the video film. According to topological criteria, there must be a saddle point between the two nodes N_{tp} and N_{ts}, as shown in Fig.6. Because of the presence of the saddle, the tip separation vortex turns its direction toward the suction side from where it stretches towards the trailing edge along the corner, see Fig.7.

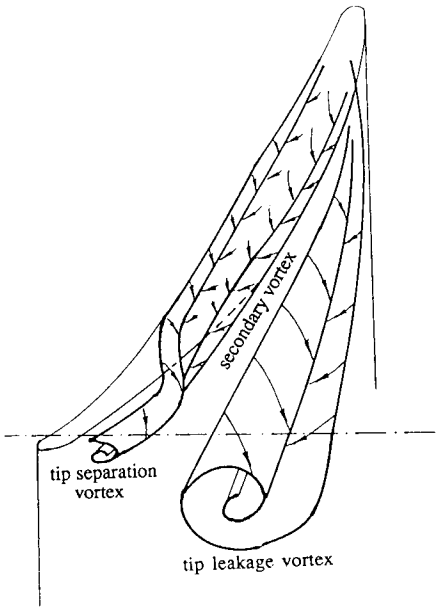

Fig.7 Schematic of the vortex structure around the tip

It is noted that Rains (1954) assumed the tip leakage flow to be two dimensional and normal to the camber line of the blade. But from the present tests, it is concluded that limiting streamlines on the blade tip surface are generally neither normal to the suction side nor to the camber line within the gap. On the stationary endwall, however, the limiting streamlines around the midchord in the pressure side are approximately normal to the pressure surface. Hence, the flow inside the tip gap is strongly three-dimensional almost over the whole chord length.

Secondary Flows and Total Pressure Losses

For a better understanding of the three dimensional flow structure, the measured data are analysed with the interactive flow visualization program CFView, developed in the Dept. of Fluid Mech., VUB (Vucinic et al., 1992). Some of the plots of the total and static pressure coefficients and secondary flow velocities are shown in Fig.8 to 11 and more details can be found in Kang (1991a).

Within the Blade Passage The velocity vector plot and static pressure contour on the blade to blade surface near the endwall at 2.0% span are shown in Fig.8. It is observed from Fig.8a that a strong secondary flow is developed near the endwall. The flow near the suction side converges to a particular line, i.e., the separation line of the tip vortex which can be identified as the line L_L of Fig.6; this separation line starts from about the first 10% chord, which is consistent with the visualization observations. Due to the development of the tip leakage vortex, a low pressure trough is formed on the endwall near the suction side around the midchord (Fig.8b). The low pressure core increases with tip gap. Associated with it, the total pressure loss reaches its high values.

Figure 9 shows the contours of total pressure loss on all the traverse planes from the leading edge to downstream of the exit at 1.0% and 2.0% tip clearances. Figure 10 shows a selection of the secondary flow vector plots for the traverse plane No.10 (88% c) and 15 (125% c) at the clearance of 1.0%. The secondary flow vectors were obtained by projecting the measured velocities on the plane normal to the flow direction at midspan at the same pitch coordinate, Kang and Hirsch

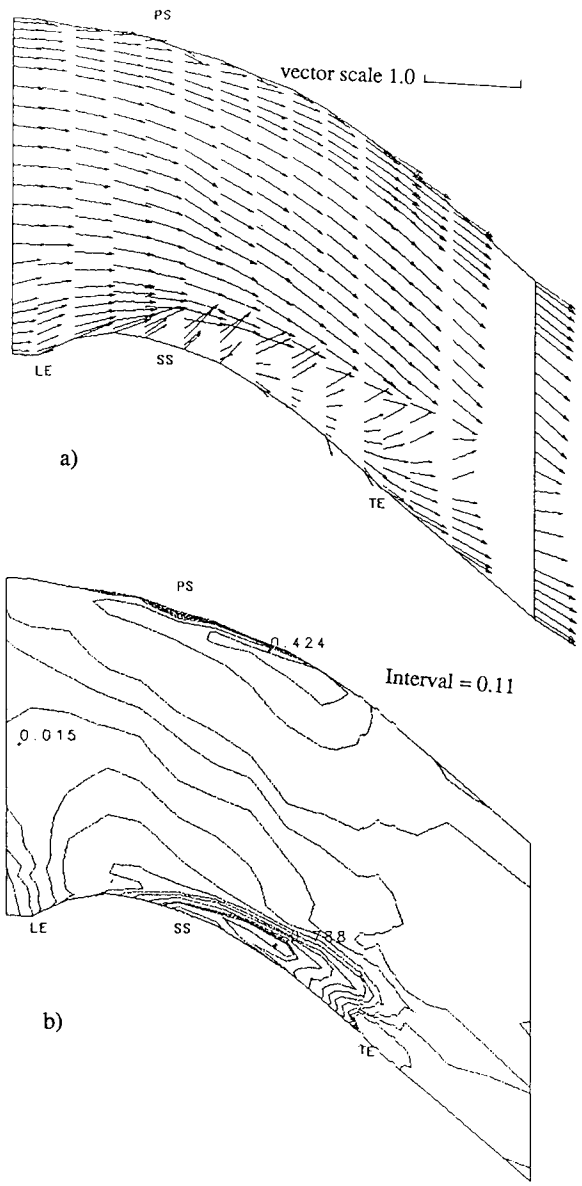

Fig.8 a) velocity vector plot and b) static pressure contour near the wall (y/l=0.02) at τ/c=0.02

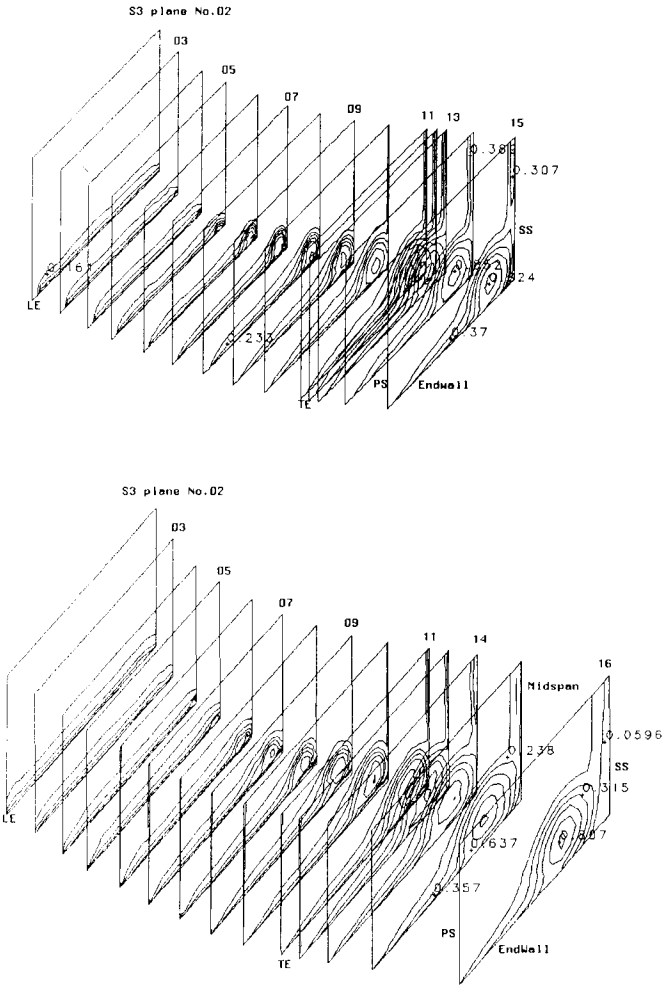

Fig.9 Contours of total pressure loss on traverse planes at a) τ/c=0.01, and b) τ/c=0.02, Interval = 0.14 in range of 0~2.4

(1991). The first impression from the plots in Fig.9 and 10 is the generation and development of the tip leakage vortex with high total pressure loss and strong rotation motion. It is seen that the isolines in the suction side corner with high values are quasi-circular and are well consistent with the rotation centre of the tip vortex. Even though the presence of the tip leakage vortex can be evidenced at about 10% chord downstream of the leading edge from the visualizations (Fig.3 and 5) and from the near wall velocity vector chart of Fig.8a, the apparent rotation or the quasi-circular isolines can be identified from the S_3 plane No.6 (44% c). Due to its very small size, more information can not be obtained near the leading edge with the present measurement method with 2.6mm five hole probe. As noted by Sjolander and Amrud (1987), the starting point of the leakage vortex at larger tip gaps is shifted axially. In the present study, the shifting is characterized by the less apparent rotation on the secondary flow plots at τ/c=2.0% compared to τ/c=1.0%.

Figure 11 shows the approximate coordinates P_y and P_z of the passage vortex core centre, defined by the distance of the rotation centre from the endwall and from the passage suction side. Those data were read from the secondary vector charts of Fig.10 in each traversed plane for different tip clearances, including the zero clearance. It is found that the tendency of the passage vortex centre in the pitchwise direction is similar for the three clearance cases in the rear half chord region. In the front half chord, however, the passage vortex in the cases with tip gap are closer to the suction side than the zero tip gap case. The reason may be that the low energy fluids of the blade pressure surface and endwall boundary layers in the pressure side corner have been driven through the tip gap to the suction side corner in the adjacent passage as observed from the visualization. As a result, the endwall boundary layer of the pressure side is thin. This can be identified from the total pressure loss coefficient contours in Fig.9. It is seen that close to the leading edge planes, the total pressure coefficient contours are basically uniform over the whole pitch for the two clearance cases. But starting from the traverse plane No.3, the loss is going to lower values in the pressure side corner but to higher values in the suction side corner. Hence the passage vortex or the rotation of the passage secondary flow shifts to the suction side.

In the spanwise direction, the vortex has almost the same height P_y near the leading edge plane. Downstream of the leading edge, the vortex trends to go up and then almost keeps at a constant height from midchord to trailing edge. It is observed in Fig.11 that the generation of the tip leakage vortex results in the passage vortex moving close to the endwall.

a)

b)

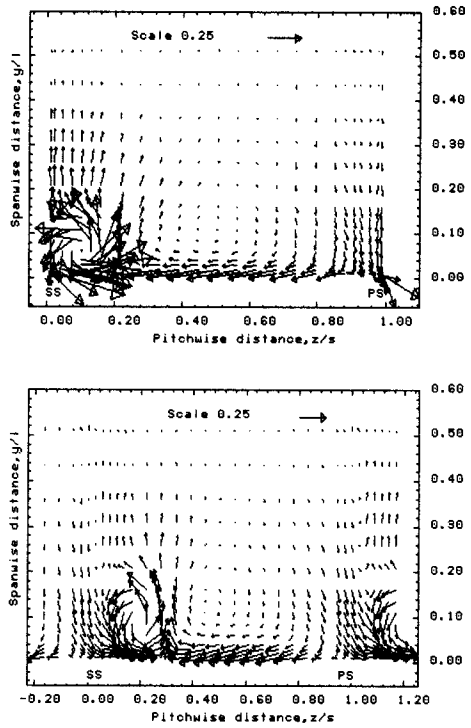

Fig.10 Secondary velocity vectors at τ/c=0.01 on traverse planes a) No.10 (88% c), and b) No.15 (150% c)

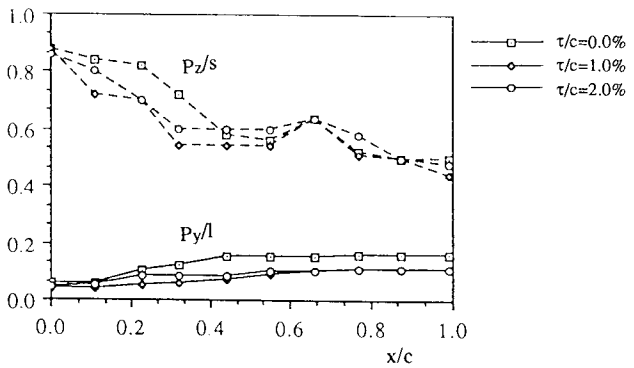

Fig.11 Position of passage vortex centre in its cross section

More evidence on the behaviour of the leakage flow can be viewed from 12, which shows the contours of total pressure losses near the pressure surface (z/s=0.98) and the suction surface (z/s=0.01). It is seen that the start of the high loss region near the suction surface (Fig.12b) just corresponds to the start of the significant decrease in the pressure side (Fig.12a). Therefore, it can be concluded that the tip leakage flow or the resulting tip leakage vortex would largely be influenced by viscous effect and depends upon the thickness of the inlet boundary layer and Reynolds number, even though the driving force may be due to inertia, as described by Rains (1954).

Figure 13 shows zooms of the secondary velocity vector in the suction side corner on the S_3 plane No.7 (55% c) and 11 (98% c) for 2.0% clearance. From this figure the tip separation and secondary vortices in the multiple vortex structure shown in Fig.7 can be evidenced. It was found from the measured secondary flow velocities

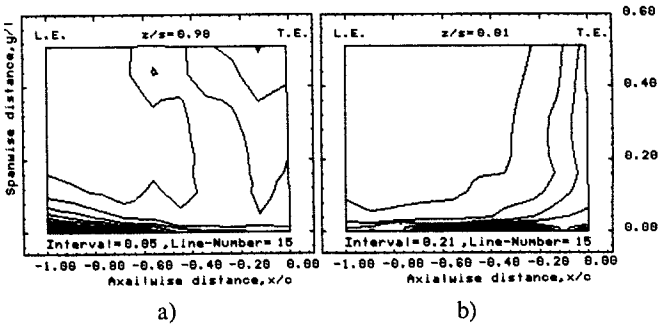

a) b)

Fig.12 Contours of total pressure losses a) near pressure surface (z/s=0.98), and b) near suction surface (z/s=0.01) at τ/c=0.01

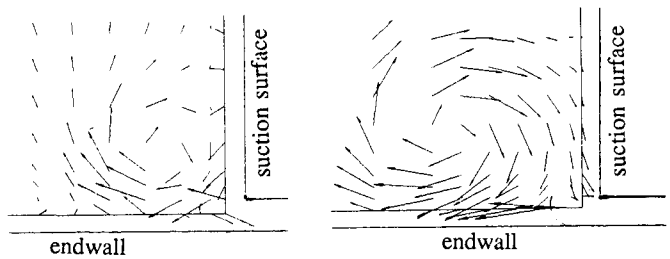

a) b)

Fig.13 Zooms of the secondary velocity vector in the suction side corner for 2.0% clearance on the S_3 planes, a) No.7 (55% c), and b) No.11 (98% c)

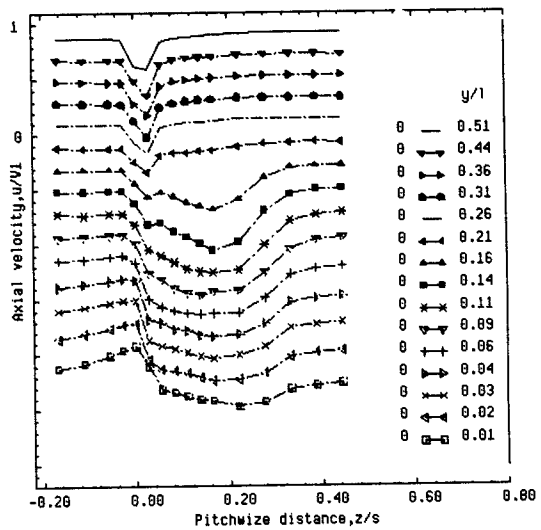

Fig.14 Spanwise development of the axial velocity on transverse plane No.14 (112.5% c) for τ/c=0.01

that in the extreme corner, a small and weak rotation in opposite sense to the tip leakage vortex exists, from the planes No.6 to 9 (Fig.13a), but in the same sense as the tip leakage vortex near trailing edge planes No.10 and 11 (Fig.13b). The rotation around the midchord is believed to be associated with the secondary vortex, but the rotation near the trailing edge to be the separation vortex, as schematically drawn in Fig.7. This means that the secondary vortex may be mixed before reaching the trailing edge, due to it is weak and opposite sense, or that due to its small size, it could not be measured with the present facility.

Behind the Passage Fig.14 shows the spanwise development of

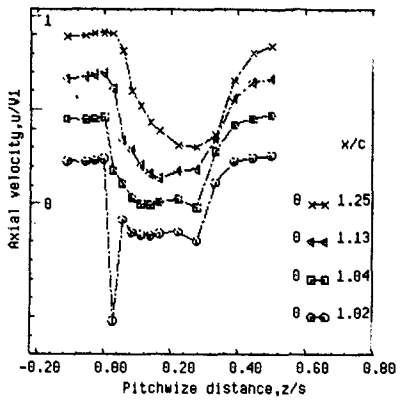

Fig.15 Axialwise development of the axial velocities near the tip leakage vortex centre at y/l=0.09 for τ/c=0.01

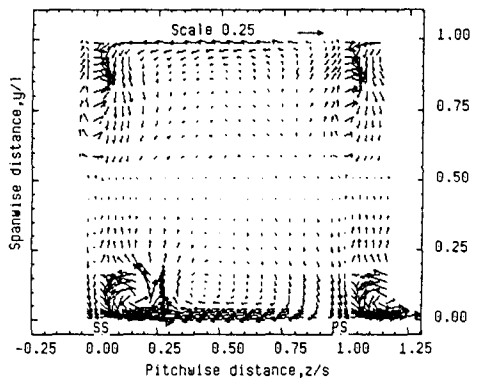

Fig.16 Full span secondary flow vectors on the traverse plane No.14 (112.5% c) for τ/c=0.01

the axial velocities on the traverse plane No.14 (112.5% chord behind the cascade) at τ/c=0.01. Figure 15 shows the axialwise development of the axial velocities near the tip leakage vortex centre at y/l=0.09 for 1.0% clearance from 2% to 25% downstream of the trailing edge. It is seen from Fig.14, also from Fig.9 and 10 that even though the tested model is a linear cascade, the wake flow is still dominated by significant three-dimensionality. With the existence of the tip clearance, the wake has been fully distorted except near midspan. The profiles in Fig.15, have two defect regions near the trailing edge; one corresponds to the blade wake, the other to the core of the tip vortex. But with the development along the streamwise direction the former tends to disappear due to the interaction between the wake and the tip leakage vortex.

The multiple tip vortex structure, i.e., the secondary vortex and the separation vortex in Fig.7, was not observable in all the downstream traverse planes. They may be mixed with or entrained into the wake and/or the tip leakage vortex, due to their small size and weak vorticities.

A measurement over the full span was also conducted in the traverse plane No.14, even though it was believed that the influence of the tip clearance is confined only within a half span. The result is shown in Fig.16 for the secondary velocity vector. It is seen that the flow features in the upper half span are fairly similar to those of the previous measurements in the lower half span with no tip gap.

Summary A weak horseshoe vortex will be generated in front of the leading edge at smaller clearance under the present conditions. In the 1.0% and 2.0% clearances, the vortex is evidenced from the probe measurements and visualizations. But with further increase of the clearance, the vortex will not occur, as observed from the visualization at 3.3% clearance.

The passage and tip leakage vortices have different properties in

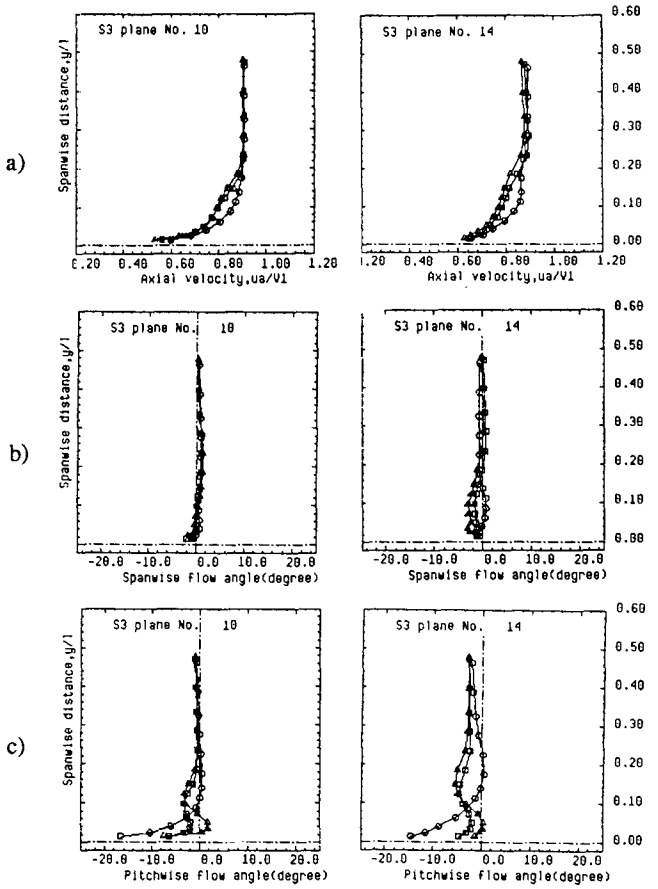

Fig.17 Pitchwise mass-averaged profile of a) axial velocities, and b) pitchwise and c) spanwise flow angles on S_3 planes No.10 (88% c) and No.14 (112.5% c)
circle -- τ/c=0.0; square -- τ/c=0.01; triangle -- τ/c=0.02

compressor cascades. The tip leakage vortex is basically formed from the low energy fluid coming from the pressure and suction surface boundary layers near the tip and from the endwall boundary layers around the tip. It has a distinctive core being seen not only from the vector plots of secondary velocity but also from the total pressure and/or the static pressure coefficient contours. For the passage vortex, the fluid rotating with it is partly viscous from the boundary layers and partly inviscid from outside of the boundary layers. Therefore, the rotation centre of the passage vortex is not always coincident with higher loss and/or lower static pressure. For turbine cascades such as those mentioned by Langston et. al. (1977) and Marchal and Sieverding (1977), the much stronger horseshoe vortex, with its pressure side leg rolling up most of the low momentum fluids in the incoming boundary layer into it, will be merged into the passage vortex in its downstream development. Thus a distinct low energy or static pressure region may exist around the passage vortex centre.

The multiple tip vortices shown in Fig.7, based on the visualizations and measurements is a first observation of this phenomenon in cascade. Even though the accuracy of the measured data in the extreme suction side corner, Fig.13, may be interfered by the solid walls, the authors believe that the multiple vortex structure shown in Fig.7 is possible and correct at least qualitatively. It is noted that Sjolander and Amrud (1987) also mentioned multiple tip vortices in a turbine cascade study. But their 'first vortex', corresponding to the secondary vortex in the present paper, has the same sense as the tip leakage vortex, which was deduced only based on their suction surface static pressure contours.

Pitchwise-Averaged Parameters

The data for each traverse plane were averaged across the pitch, taking

the definitions given in Kang (1990). Figure 17 shows a selection of the axial velocities, and pitchwise and spanwise flow angles in the traverse planes No.10 and 14. With the present test conditions, moderate turning angle and low flow speed, the averaged axial velocity profiles on each traverse plane in the front half chord are similar to each other for all three cases, except for a small difference in magnitude. But the averaged pitchwise flow angles show significantly less overturning near the endwall for the cases with tip clearance, starting from the S_3 plane No.3 (11% chord). The lower overturning is attributed to the opposite actions of the tip leakage vortex and the passage vortex.

From midchord to downstream, the pitchwise mass-averaged axial flow velocity profiles for 1.0% and 2.0% tip gaps (Fig.17a) are not still parabola-like but have two turning points along the profiles, which is related to the influence of the wake-like profile (see Part II of this paper) in the tip vortex core and the wake flow. With the development of the tip leakage vortex, the averaged flow angle profile (Fig.17c) shows overturning, underturning and overturning from midspan to the wall. The overturned region farthest away from the wall is most probably associated with the passage secondary flow, i.e. the rotation of the passage vortex. But the under- and over-turning regions near the wall are related to the opposite rotation of the tip leakage vortex and the passage vortex. The underturning increases and the overturning decreases with increasing tip gap, which is consistent with the increase of the circulation of the tip vortex (see Part II of this paper). Although there are significant spanwise flows in the suction side corner and inside the wake, the pitchwise mass-averaged spanwise flow angles (Fig.17b) are quite small, especially inside the passage. It is found that behind the cascade, the averaged spanwise flow angle profile is bent and has its extreme value near the endwall. The extreme value is positive for the zero tip clearance but negative for the both tip clearances. The negative value increases with increasing tip gap.

Conclusions

The three dimensional flow in a linear compressor cascade with 1.0, 2.0 and 3.3% clearances has been discussed in this paper, and the following conclusions are drawn:

A weak horseshoe vortex is formed from the blade leading edge at small clearance. In addition to the normally known tip leakage vortex, two other small vortices were observed in the tip region; one of them was rolled up by the flow separated from the pressure side edge; the other was from the suction side edge. Hence the flow inside the gap is fully three-dimensional almost over the whole chord.

The tip leakage vortex had a quasi-circular core with high total pressure loss and low static pressure value. The core of the passage vortex, however, was not accompanied by the occurrence of high loss and low static pressure.

The generation of the tip leakage vortex resulted in the passage vortex moving close to the endwall and to the suction side of the passage.

Even in the linear cascade, the 2-D blade surface pressure is not the simple driving force of the leakage flow, The motion of the tip vortex arouses a strong reloading by which the leakage flow is reinforced.

The pitchwise mass-averaged profiles, with and without tip clearance, were basically the same upstream of midchord for all the parameters, but were significantly different downstream of midchord.

References

Bindon, J. P., 1986, "Visualisation of Axial Turbine Tip Clearance Flow Using a Linear Cascade," CUED/A-Turbo/TR 122.

Bindon, J. P., 1986, "Pressure and Flow Field Measurements of Axial Turbine Tip Clearance Flow in a Linear Cascade," CUED/A-Turbo/TR 123.

Chen, T. G., Greitzer, M. E., Tan, C. S., and Marble, F. E., 1991, "Similarity Analysis of Compressor Tip Clearance flow Structure, ASME J. of Turbomachinery," Vol.113, pp.260-271.

Davino, R., and Lakshminarayana, B., 1982, "Turbulence Characteristics in the Annulus-Wall Boundary Layer and Wake Mixing Region of a Compressor Rotor Exit," ASME J. of Eng. for Power, Vol.104, No.3, pp.561-570.

Dring, R. P., Joslyn, H. D., and Hardin,L. W., 1982, "An Investigation of Axial Compressor Rotor Aerodynamics," ASME J. of Eng. for Power Vol.104, No.1, pp.84-96.

Graham, J. A. H., 1986, "Investigation of a Tip clearance Cascade in a Water Analogy Rig," ASME J. of Eng. for Gas Turbines and Power, Vol.108, pp.38-46.

Hirsch, C., and Kool, P., 1977, "Measurement of the three Dimensional Flow Field Behind an Axial Compressor Stages," ASME J. of Eng. for Power, Vol.99, No.2, pp.168-180.

Hunter, I. H., and Cumpsty, N. A.,1982, "Casing Wall Boundary Layer Development Through an Isolated Compressor Rotor," ASME Paper No.82-GT-18.

Inoue, M., and Kuroumaru, M., 1984, "Three-Dimensional Structure and Decay of Vortices Behind an Axial Flow Rotation Blade Row," ASME J. of Eng. for Gas Turbines and Power, Vol.106, pp.561-569.

Inoue, M., and Kuroumaru, M., 1989, "Structure of Tip Clearance Flow in an Isolated Axial Compressor Rotor," ASME J. of Turbomachinery Vol.111, pp.250-256.

Inoue, M., Kuroumaru, M., Iwamoto, T., and Ando, Y., 1991, "Detection of a Rotating Stall Precursor in Isolated Axial Flow Compressor Rotors," ASME J. of Turbomachinery Vol.113, pp.281-289.

Joslyn, H. D., and Dring, R. P., 1985, "Axial Compressor Stator Aerodynamics," ASME J. of Eng. foe Gas Turbines and Power, Vol.107, pp.485-493.

Kang, S., 1989, "Five-Hole Probe Calibration," Vrije Universiteit Brussel, Dept. of Fluid Mechanics, Report No.VUB-TN-43.

Kang, S., 1990, "3-D Flows in a Linear Compressor cascade at design conditions," Vrije Universiteit Brussel, Dept. of Fluid Mechanics, Report No.VUB-TN-44.

Kang, S., 1991a, "Experimental Study on the Three Dimensional Flow Within Compressor Cascade with Tip Clearances," Vrije Universiteit Brussel, Dept. of Fluid Mechanics, Report No.VUB-TN-45.

Kang, S., 1991b, "Topological Analysis on the Three Dimensional Flow in a Linear Compressor Cascade with Tip Clearance," Vrije Universiteit Brussel, Dept. of Fluid Mechanics, Report No.VUB-TN-46.

Kang, S., and Hirsch, Ch., 1991, "Three Dimensional Flows in a Linear Compressor cascade at design conditions," ASME paper No.91-GT-114.

Kang, S., and Hirsch, Ch., 1992, "Experimental Study on the Three Dimensional Flow within a Compressor Cascade with Tip Clearance: Part II -- The Tip Vortex," ASME paper, this issue.

Kool, P., De Ruyck, J., and Hirsch, C., 1978, "The Three-Dimensional Flow and Blade Wake in an Axial Plane Downstream of an Axial Compressor Rotor," ASME Paper No.78-GT-66.

Lakshminarayana, B., 1970, "Method of Predicting the Tip Clearance Effects in Axial Flow Turbomachinery," ASME J. of Basic Eng., Vol. 92, pp.467-480.

Lakshminarayana, B., and Poncet, A., 1974, "A Method of Measuring Three-Dimensional Wakes in Turbomachinery," ASME J. of Fluids Eng., Vol.96, No.2, pp.87-91.

Lakshminarayana, B., Pouagare, M., and Davino, R., 1982, "Three Dimensional Flow Field in the Tip Region of a Compressor Rotor Passage, Part I: Mean Velocity Profiles and Annulus Wall Boundary Layer," J. of Eng. for Power, Vol.104, No.4, pp 760-771.

Lakshminarayana, B., Zhang, J., and Muthy, K. N. S., 1987, "An Experiment Study on the Effects of Tip Clearance on Flow Field and Losses in Axial Flow Compressor Rotor," ISABE 87-7045, pp 273-290.

Langston, L. S., Nice, M. L., and Hooper, R. M., 1977, "Three-Dimensional Flow Within a Turbine Blade Passage," ASME J. of Eng. for Power, Vol.99, No.1, pp.21-28.

Marchal, P., and Sieverding, C. H., 1977, "Secondary Flow Within Turbomachinery Bladings,"Secondary Flows in Turbomachines,AGARD CP-214.

Moore, J., and Tilton, J. S., 1988, "Tip Leakage Flow in a Linear Turbine Cascade," J. of Turbomachinery, Vol. 110, pp.18-26.

Prasad, C. R. K., 1977, "Tip Clearance Effect in Axial Flow Turbomachines," Indian Institute of Science, Report No. ME-TURBO-1-77.

Rains, D. A., 1954, "Tip Clearance Flow in Axial Compressors and Pumps," California Institute of Technology, Mech. Eng. Laboratory, Report 5.

Sjolander, S. A., and Amrud, K. K., 1987, "Effects of Tip Clearance on Blade Loading in a Planar Cascade of Turbine Blades," ASME J. of Turbomachinery, Vol.109, pp.237-245.

Storer, J. A., and Cumpsty, N. A., 1991, "Tip Leakage Flow in Axial Compressors," ASME J. of Turbomachinery, Vol.113, pp.252-259.

Vucinic, D., Pottiez, M., Sotiaux, V., and Hirsch, Ch., 1991, "CFView, An Advanced Interactive Visualization System Based on Object-Oriented Approach," AIAA-92-0072.